Northumbria Research Link

**Geoscientific
Model Development**

Pliocene Model Intercomparison Project (PlioMIP): experimental design and boundary conditions (Experiment 1)

**A. M. Haywood[1], H. J. Dowsett[2], B. Otto-Bliesner[3], M. A. Chandler[4,5], A. M. Dolan[1], D. J. Hill[6], D. J. Lunt[7,8],
M. M. Robinson[2], N. Rosenbloom[3], U. Salzmann[9], and L. E. Sohl[4,5]**

[1]School of Earth and Environment, University of Leeds, Woodhouse Lane, Leeds, LS2 9JT, UK
[2]Eastern Geology and Paleoclimate Science Center, US Geological Survey, MS926A, 12201 Sunrise Valley Drive,
Reston, VA 20192, USA
[3]CCR, CGD/NCAR, P.O. Box 3000, Boulder, CO 80307-3000, USA
[4]Center for Climate Systems Research, Columbia University, 2880 Broadway, New York, NY, 10025, USA
[5]NASA Goddard Institute for Space Studies, New York, NY, USA
[6]British Geological Survey, Keyworth, Nottingham, NG12 5GG, UK
[7]School of Geographical Sciences, University of Bristol, University Road, Bristol, BS8 1SS, UK
[8]British Antarctic Survey, High Cross, Madingley Road, Cambridge, Cambs, CB3 0ET, UK
[9]School of Applied Sciences, Northumbria University, Newcastle upon Tyne, NE1 8ST, UK

Abstract. In 2008 the temporal focus of the Palaeoclimate Modelling Intercomparison Project was expanded to include a model intercomparison for the mid-Pliocene warm period (3.29–2.97 million years ago). This project is referred to as PlioMIP (Pliocene Model Intercomparison Project). Two experiments have been agreed upon and comprise phase 1 of PlioMIP. The first (Experiment 1) will be performed with atmosphere-only climate models. The second (Experiment 2) will utilise fully coupled ocean-atmosphere climate models. The aim of this paper is to provide a detailed model intercomparison project description which documents the experimental design in a more detailed way than has previously been done in the literature. Specifically, this paper describes the experimental design and boundary conditions that will be utilised for Experiment 1 of PlioMIP.

1 Introduction

1.1 The mid-Pliocene warm period

The mid-Pliocene warm period (MPWP) is defined by the United States Geological Survey's PRISM Group (Pliocene Research Interpretation and Synoptic Mapping; http://geology.er.usgs.gov/eespteam/prism/index.html) as the interval between 3.29 and 2.97 Ma (according to the

geomagnetic polarity timescale of Berggren et al., 1995), lying between the transition of oxygen isotope stages M2/M1 and G19/G18 (Shackleton et al., 1995), in the middle part of the Gauss Normal Polarity Chron (Dowsett et al., 1999). The "Time Slab" represents a climatically distinct period during the Pliocene when Earth's climate was, on the whole, warmer than present (Dowsett et al., 1999; Dowsett, 2007a; see Fig. 1).

The interval was originally selected as the basis for a Pliocene palaeoclimate reconstruction for several reasons. Downcore studies of marine microfossils had established this period as a time of warmer than modern climate (i.e. Dowsett and Poore, 1991; Cronin, 1991; Barron, 1992; Dowsett et al., 1992; Dowsett and Loubere, 1992; etc.). Several studies of Pliocene high latitude vegetation also suggested substantial warmth relative to today (i.e. Matthews and Ovenden, 1990; Webb and Harwood, 1991). This interval occurs prior to the major oxygen isotope excursion representing the major climate step toward modern conditions (polar fronts strengthened and glacial-interglacial variation intensified (Sancetta and Silvestri, 1986; Raymo et al., 1989; Hodell and Ciesielski, 1991). The PRISM interval is long enough to be reliably identified and correlated between marine records based upon a suite of methods: biochronology, magnetic stratigraphy, stable isotope stratigraphy. Finally, this interval is the geologically most recent interval exhibiting significant warmth but in range of multiple temperature proxies involving extant fauna and flora.
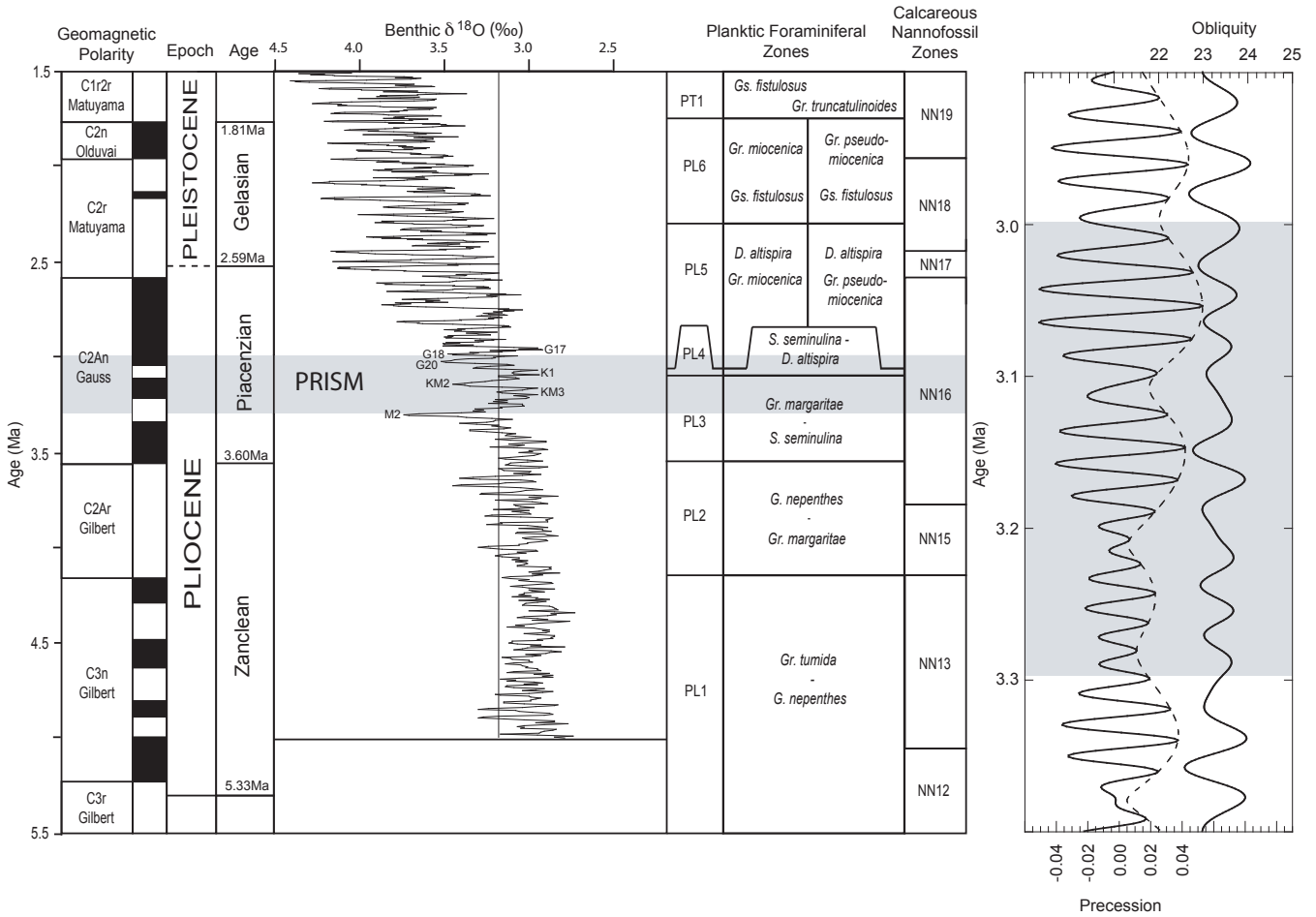
Fig. 1. Position of the MPWP time slab (shaded band) relative to geomagnetic polarity, magnetic reversals (black and white boxes), Pliocene Stages, oxygen isotope stratigraphy, planktic foraminiferal zones, calcareous nannofossil zones and orbital geometry (modified from Dowsett and Robinson, 2006).

The MPWP has been the subject of intense study for the last two decades. There are many reasons for this, but an important driver has been our desire to understand the dynamics of past warm climates as a potential guide to understanding climate change in the future (Haywood et al., 2009). The MPWP is well suited to this task. The climatic signal (change from modern) is sufficiently large, for many geographical regions, to be differentiated from the noise generated by the uncertainties and limitations inherent in the techniques used for palaeoclimatic/palaeoenvironmental reconstruction. The interval was the last time in Earth history when global temperatures were significantly warmer than modern, over a period longer than any Quaternary interglacial. It is unique in that continental configurations were relatively unchanged from today, and geological proxies are superior to those of preceding warm periods due to improved geographic coverage, more reliable biota-environment correlations and higher resolution stratigraphy (Dowsett, 2007a).

Although mean conditions during the MPWP were distinctly warmer than mean conditions during any 300 kyr interval since, there was a high degree of climate variability (e.g. Lisiecki and Raymo, 2005). Reconstructions of sea surface temperature (SST) carried out by the PRISM group are designed to capture "mean interglacial conditions" during the 3.29–2.97 million year interval. Thus a warm-peak-averaging (WPA) technique was employed to extract the warm phase of climate from SST time series (see Dowsett and Robinson, 2006; Dowsett, 2007a). Warm peak averaging, pioneered by Dowsett and Poore (1990), attempts to determine the average peak warming during the MPWP. Only estimates meeting pre-set quality control criteria are used (see Dowsett, 2007a). A warm peak is defined as a temperature warmer than the estimates surrounding it in a stratigraphic sequence. Thus, all warm peaks are defined, those not meeting quality control are excluded, and the remainders are averaged (see Sect. 3.3 for further details).

1.2 Palaeoclimate modelling, PMIP and PlioMIP

General Circulation Models (GCMs) are now routinely used to simulate and predict Earth's present and future climate (e.g. Solomon et al., 2007). Although there is broad agreement among the models, there are also significant differences in the details of their predictions (Randall et al., 2007). Numerous palaeoclimate simulations have been conducted for various intervals in Earth History (e.g. Kutzbach and Otto-Bliesner, 1982; Barron and Washington, 1982; Valdes and Sellwood, 1992; Kim and Crowley, 2000; DeConto and Pollard, 2003; Huber and Caballero, 2003; Haywood et al., 2007; Sohl and Chandler, 2007). In part, these studies are being carried out in an effort to determine whether or not GCMs can successfully retrodict climatic conditions significantly different from present day. Through comparison with geological proxy data, such studies may provide us with more confidence in climate model simulations for the future (Williams et al., 2007 and chapters therein). However, it has been the norm in palaeoclimate modelling studies for only a single model to be used in any one study, meaning the degree to which the results are model dependent is often not addressed.

Exceptions to this norm are the modelling studies carried out as part of the Palaeoclimate Modelling Intercomparison Project (PMIP), which was initiated in order to co-ordinate and encourage the systematic study of climate models and to assess their ability to simulate large differences of climate that occurred in the past (e.g. Joussaume and Taylor, 1995; Hoar et al., 2004; Zheng et al., 2008). It has also served to encourage the preparation of global reconstructions of palaeoclimates that can be used to evaluate climate models (e.g. Prentice and Webb, 1998). The temporal focus of the studies carried out by PMIP phases I and II was restricted to the Last Glacial Maximum and the mid-Holocene climatic optimum, for which detailed reconstructions of palaeoenvironmental conditions exist in a suitable format for integration with climate models. However, at a meeting to discuss the scientific agenda for PMIP phase III, held in September 2008 in Boulder Colorado (a summary of which can be found in Otto-Bliesner et al., 2009), it was decided to expand the temporal range of PMIP to include the 8.2 kyr event, the Last Interglacial and the Mid-Pliocene Warm Period (MPWP).

For the initial phase of the MPWP model intercomparison (hereafter referred to as PlioMIP (Pliocene Model Intercomparison Project) two experiments were agreed upon. The first is an experiment using atmosphere-only climate models (hereafter referred to as Experiment 1), whilst the second experiment (hereafter referred to as Experiment 2) will utilise coupled ocean-atmosphere climate models. Both experiments use versions of the US Geological Survey's PRISM Group boundary condition data sets. This Special Issue of Geoscientific Model Development represents the first set of co-ordinated publications from the PlioMIP project. It describes (a) the chosen experimental design for Experiments 1

and 2, (b) includes a detailed description of the boundary conditions used in both experiments, and (c) presents contributions from each participating model group which describe how the boundary conditions were implemented into the different climate models, along with the basic results from the experiments themselves. This detailed record for the rationale and specifics of the experimental design, construction of the boundary conditions data sets, and critically, how these were implemented into each climate model, will provide an invaluable reference when the intercomparison phase of PlioMIP is reached, helping the PlioMIP/PMIP community to understand more easily the differences which will inevitably be observed between MPWP simulations. The purpose of this paper is to describe the experimental design and boundary conditions for PlioMIP Experiment 1.

2 Experimental design – Experiment 1

2.1 Integration length, atmospheric gasses/aerosols, solar constant/orbital configuration

The experimental design for Experiment 1 is summarised in Table 1. The experiment integration length was set to 50 years. Given the specified SSTs and quick response time of the atmosphere, this integration length will enable even the slowest responding elements of the system in an AGCM experiment, such as deep soil moisture, to reach full equilibrium. The first 20 years of the simulations will be considered spin-up. The concentration of CO_2 in the atmosphere was set to 405 ppmv which is a little more than the average range ($\sim$360–380 ppmv) of palaeo CO_2 indicated by available proxy data (Kürschner et al., 1996; Raymo et al., 1996). The CO_2 value was chosen to also account for possible additional contributions to greenhouse warmth from non-CO_2 greenhouse gases such as methane, for which we have no proxy record in the Pliocene, a possibility which is consistent with the coupled nature of variation in CO_2 and methane concentrations in Quaternary ice core records (e.g. Loulergue et al., 2008; Lüthi et al., 2008). In the absence of any adequate proxy data, all other trace gases and aerosols were specified to be consistent with the individual group's pre-industrial control experiments, as was the solar constant.

The orbital configuration was specified as the same as each participating group's pre-industrial control run. The PRISM3D data set of mid-Pliocene boundary conditions represents an average of the warm intervals during the time slab (3.29–2.97 million years) rather than a discreet time slice, making it challenging to prescribe an orbital configuration which is representative of the entire $\sim$300 000 year interval. Furthermore, it is difficult to provide an average insolation forcing at the top of the atmosphere in some climate models, with some models requiring specific values for eccentricity, obliquity and precession. Therefore, PlioMIP decided to specify a modern orbital configuration, even though available astronomical solutions (e.g. Laskar et al., 2004) indicate

Table 1. Experimental design – PlioMIP Experiment 1.

Model Coupling				
Atmosphere-Only				
Integration Length				
50 years				
Oceans				
Ocean Mode			Deep Ocean Input	
Specified SST Climatology			none	
Preferred Boundary Conditions				
Land/Sea Mask	Topography	Ice Sheets	Vegetation	SST
PRISM3D (land_fraction_v1.1)	PRISM3D (topo_v1.1*)	PRISM3D (biome_veg_v1.3 or mbiome_veg_v1.3)	PRISM3D (biome_veg_v1.3 or mbiome_veg_v1.3)	PRISM3D (PRISM3_SST_v1.1*)
Alternate Boundary Conditions				
Land/Sea Mask	Topography	Ice Sheets	Vegetation	SST
Local modern land/sea mask	PRISM3D (topo_v1.4*)	PRISM3D (biome_veg_v1.2 or mbiome_veg_v1.2)	PRISM3D (biome_veg_v1.2 or mbiome_veg_v1.2)	PRISM3D (PRISM3_SST_v1.3*)
Greenhouse Gases				
CO_2	N_2O	CH_4	CFCs	O_3
405 ppm	As Pre-Ind Control	As Pre-Ind Control	As Pre-Ind Control	As Pre-Ind Control
Solar Constant				
As Pre-Ind Control				
Aerosols				
As Pre-Ind Control				
Model Spin-up				
Documented by individual groups				
Orbital Parameters				
As Pre-Ind Control				

* Applied as an anomaly to control experiment data sets used by each participating group rather than as an absolute.

that this may not provide the most representative mean orbital forcing for the MPWP (Fig. 2). However, modern orbit is close to the average MPWP forcing at 65° N in July, which is thought to be an important region/time for determining the global response to orbital forcing.

2.2 Implementation of sea-surface temperatures and topography as an anomaly

To ensure that the climate anomalies (mid-Pliocene minus present day) from all PlioMIP climate models are directly comparable, i.e. that they reflect differences in the models themselves rather than the differences of modern boundary conditions, it was decided to implement both the Pliocene topography and SSTs as an anomaly to whatever standard modern SST and topographic data set is used by each mod-

elling group in their own model. To create the Pliocene SST/topography the difference between the PRISM_Pliocene and PRISM_Modern topography/SST will be calculated and added to the modern SST and topographic data sets each participating modelling group employs.

Such that:

Topo_Plio = (Topo_Plio_PRISM3D – Topo_Modern_PRISM3D) + Topo_Modern_Local

and

SST_Plio = (SST_Plio_PRISM3D – SST_Modern_PRISM3D) + SST_Modern_Local

However, when using such a method a potential mismatch between mid-Pliocene and modern topography land-sea masks is possible. This will be overcome by using absolute Pliocene topography/SST in regions where no mod-
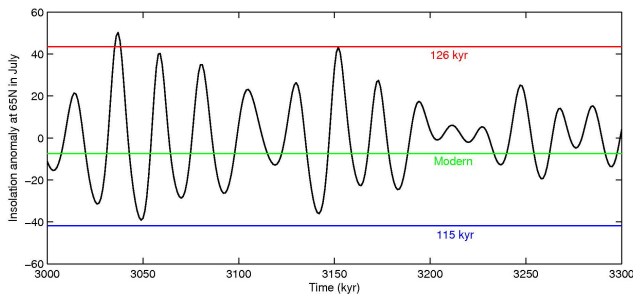
Fig. 2. Calculated insolation anomaly at the top of the atmosphere (TOA) at 65° N in July for the interval 3.3 to 3 million years ago derived from the Laskar04 solution (Laskar et al., 2004). Insolation values for the modern, 126 kyr (peak of the Last Interglacial) and 115 kyr (Last Glacial Inception Period) are added for reference.

PRISM Fractional Grid Data:

Fig. 3. Schematic representation of the PRISM3D/PlioMIP fractional grid data approach.

ern data is given (such as for the Pliocene topography in the Hudson Bay region). Modern SST is projected on the same Pliocene grids (preferred and alternate) to make anomalies easier to generate.

## 2.3 Adoption/availability of a "preferred" and "alternate" experimental design

Two boundary condition data packages are available – "preferred" and "alternate". Both data packages are provided on the PlioMIP website (http://geology.er.usgs.gov/eespteam/prism/prism_pliomip_data.html) and are provided as supplementary information to this paper. The preferred data package requires the ability to change the models land/sea mask to a mid-Pliocene configuration. The alternate data package, with a modern land/sea configuration, is provided in order to maximise the potential number of participating groups in PlioMIP, since it is difficult in some climate models to successfully alter the land/sea mask. Groups that are not able to change their land/sea mask were asked to use their own modern land/sea mask. However, a PRISM3D/PlioMIP modern land/sea mask is provided in the alternate package to help guide the implementation of mid-Pliocene topography and vegetation, etc. into different climate models.

3 Description of boundary conditions (PRISM3D)

3.1 Land-sea mask and topography (outside of ice-sheet regions)

The PRISM3D/PlioMIP land/sea mask and topographic reconstruction is provided in both netCDF format and as an Excel spreadsheet at a 2°×2° resolution. In contrast to the land/sea mask presented in older PRISM2 reconstruction of Dowsett et al. (1999), the PRISM3D land/sea mask is fractional. Continental and oceanic regions are 100% land and ocean respectively, but the margin between these areas is fractional. Areas with only land are given land cover (biome
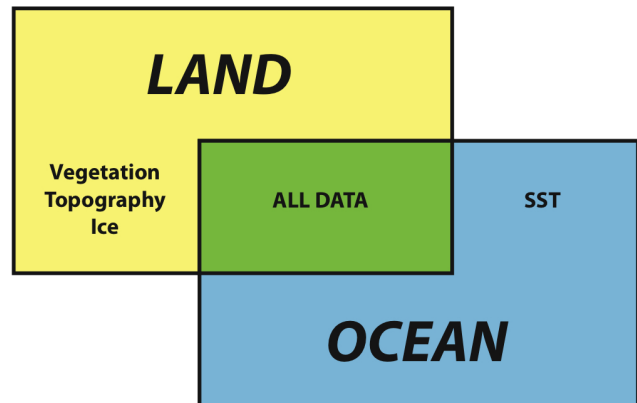
and mega-biome see Sect. 3.6) classification, and topography. Ocean only areas have ocean temperature. Fractional land-sea regions (coastal areas) are given all relevant data types. A representation of the PRISM3D/PlioMIP fractional data system is provided in Fig. 3.

In PRISM3D global sea-level is estimated to be 25 m higher than modern. This is consistent with evidence from palaeoshorelines (e.g. the Orangeburg Scarp along the US Atlantic Coastal Plain; Dowsett and Cronin, 1990) and the results of numerical ice sheet models (Hill et al., 2007; Hill, 2009; Pollard and DeConto, 2009; see Sect. 3.3).

The fractional land/sea mask and topographic reconstruction is shown in Fig. 4. To create a coastline which reflected a 25 m sea-level rise, an ocean mask derived from the ETOPO5 data set (NOAA, 1988) was superimposed over the modern continental outline (Fig. 5). The Hudson Bay was in-filled at low elevation due to this feature being derived largely from glacial erosion during the Pleistocene. The West Antarctic Ice Sheet is absent (Pollard and DeConto, 2009; see Sect. 3.3) which creates waterways in locations where the current bed-rock elevation is less than 25 m higher than modern sea-level.

The basic PRISM3D/PlioMIP topographic reconstruction is based on the Pliocene palaeogeography of Markwick (2007), which introduces greater detail in the topography (especially in the 0–500 m range) than was available in the PRISM2 topographic data set (Thompson and Fleming, 1996; Dowsett et al., 1999). Topography (outside of ice sheet regions) incorporates the following changes compared to the previous topographic data set presented in the PRISM2 reconstruction of Dowsett et al. (1999). Specifically, in PRISM2 the western cordillera in northern South America and in the Rocky Mountains/Colorado Plateau was reduced by 2000 and 1500 m, respectively, to ~50% of the modern
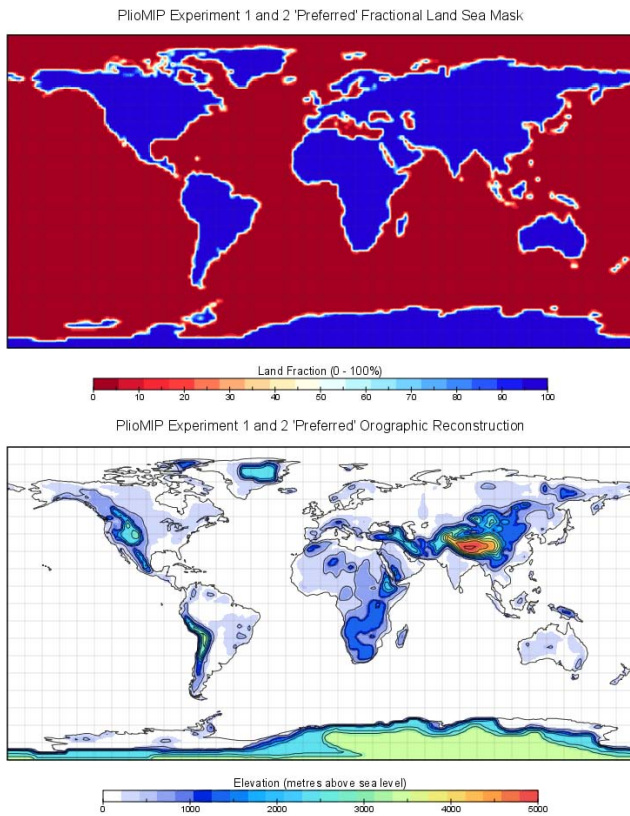
Fig. 4. "Preferred" fractional land/sea mask (top) with mid-Pliocene orography (bottom) for use in Experiments 1 and 2 (Sohl et al., 2009). Basic palaeogeographic reconstruction derived from Markwick (2007), modified to account for ice sheet model-predicted ice sheet extent and height above sea-level (see Sect. 3.2).
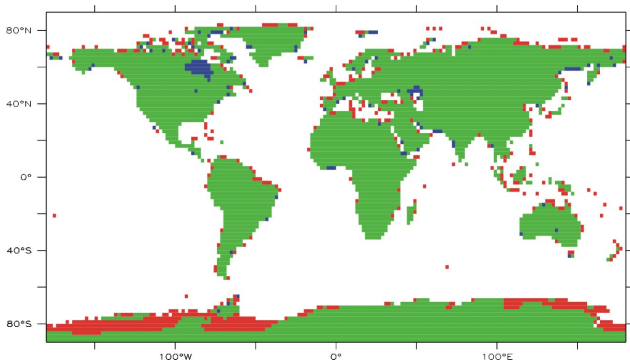
Fig. 5. Differences in "preferred" mid-Pliocene and modern land sea mask with red cells highlighting additional land points in the modern and blue cells highlighting additional land points for the mid-Pliocene.

elevation (Thompson and Fleming, 1996). More recent studies by Garzione et al. (2006), Ghosh et al. (2006), Rowley and Garzione (2007) and McMillan et al. (2006) suggest that such a large reduction in elevation is unlikely at ca. 3 Ma, thus the Rocky Mountains and Andes are specified at approx-
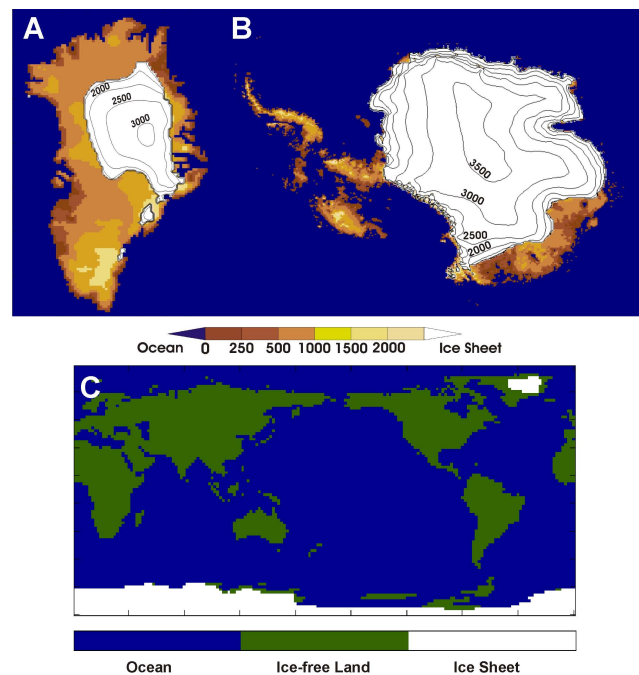
Fig. 6. PRISM3D mid-Pliocene warm period ice sheet reconstructions (Hill et al., 2007; Hill, 2009; Salzmann et al., 2008) for the Greenland (A) and Antarctic (B) ice sheets and their extent on the PRISM3D global grid (C).

imately their current elevations in PRISM3D. Further details of the PRISM3D/PlioMIP land/sea mask and topographic reconstruction can be found in Sohl et al. (2009).

3.2 Ice-sheet height and extent

The direct geological evidence for ice sheets in the Pliocene is sparse and, when inferences are made about the wider cryosphere, seemingly inconsistent. Previous iterations of the PRISM data set (i.e. PRISM2) included ice sheet reconstructions based on sea-level data and marine isotope ratios and idealised ice sheet modelling (Dowsett and Cronin, 1990; Dowsett et al., 1999). Whilst this provided a reasonable initial approximation, the uncertainties in the data, and thus in the reconstructions themselves, are large (Krantz, 1991). Furthermore, while overall ice volumes can be estimated from proxy data, the proxies can not differentiate between different potential ice sheet locations.

New ice sheet estimates were produced from high-resolution ice sheet model experiments performed with the British Antarctic Survey Ice Sheet Model (BASISM), utilising Hadley Centre GCM (Gordon et al., 2000) climatologies produced with PRISM boundary conditions (Hill et al., 2007; Hill, 2009; Fig. 6). The climate simulation chosen for these ice sheet reconstructions is the same as that chosen for the PRISM3D vegetation reconstruction (Salzmann et al., 2008; see Sect. 3.5).
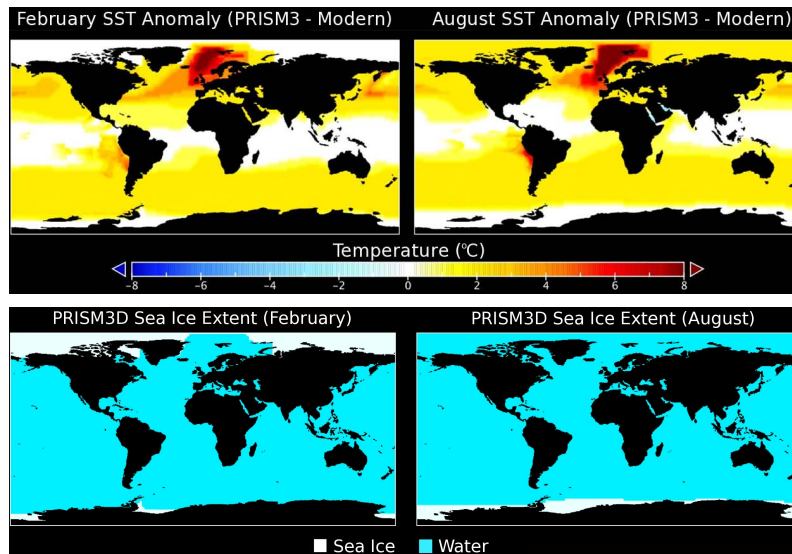
Fig. 7. PRISM3D SST anomaly for February (top left) and August (top right). PRISM3D sea-ice extent for February (bottom left) and August (bottom right).

The PRISM3D ice sheet reconstruction shows significant changes from the modern ice sheets over Greenland and Antarctica. On Greenland, the ice sheet extent is much reduced, with ice restricted to the high-altitude regions of East Greenland. In East Antarctica, while large portions of the ice sheet show little change or a small increase in surface altitude, significant ice-sheet retreat occurs in the Wilkes and Aurora Sub-glacial basins. These areas are currently below sea-level and largely unconstrained by topography, so provide a good candidate for East Antarctic Ice Sheet retreat. West Antarctica has not been modelled in these experiments, as all the major mechanisms of marine ice-sheet retreat have yet to be robustly included in ice sheet models (Vieli and Payne, 2005). However, recent ANDRILL core data and ice sheet modelling (Naish et al., 2009; Pollard and DeConto, 2009) suggests that, at least in the warmest periods of the Pliocene, there was no ice present in West Antarctica. Combining this assumption with our models of Greenland and East Antarctica predicts ice sheet retreat of over 22 m sea-level equivalent, in good agreement with eustatic sea-level estimates.

3.3 Sea-surface temperatures

The PRISM3D sea-surface temperature field is presented on the same $2° \times 2°$ resolution fractional grid described in Sect. 3.1 as a series of 12 monthly SST fields in netCDF or Excel format. PRISM3D SST differs from PRISM2 SST (Dowsett et al., 1999; Dowsett, 2007a) by taking into account data from more localities, particularly in the equatorial Pacific (Dowsett, 2007b; Dowsett and Robinson, 2009) and North-eastern Atlantic/Arctic regions (Robinson, 2009; Robinson et al., 2008; Dowsett et al., 2009a, b). In addi-

tion, PRISM3D incorporates for the first time multiple temperature proxies (multivariate analysis of fossil planktonic foraminfers, ostracods, and diatoms as well as Mg/Ca and alkenone unsaturation index palaeothermometry) which provide greater overall confidence in the SST fields.

In order to provide a single temperature value at each locality PRISM uses a warm-peak averaging (WPA) technique whereby time-series data are analysed and warm peaks are averaged. Details of the technique can be found in Dowsett and Poore (1991), Dowsett (2007a) and Dowsett and Robinson (2006). A late Pleistocene analogy would be to average the temperatures from peak interglacials at marine isotope stages 5e, 7 and 9 to generate a single representative "interglacial temperature estimate" for a particular location.

Once February (August) temperature estimates are determined for each locality using WPA, the estimates are subtracted from modern temperature (Reynolds and Smith, 1995) to create SST anomalies (Figs. 7 and 8). These anomalies are superimposed on a modern SST map for February (August) and the anomaly patterns are extrapolated globally using the distribution of actual data points and the modern SST field and its gradients as a guide. This new anomaly field is then added to the modern SST fields of Reynolds and Smith (1995) (= SST_Modern_PRISM3D; Sect. 2.2 above) to create Pliocene February (August) SST (= SST_Plio_PRISM3D; Sect. 2.2 above).

In many regions of the present day ocean, the annual SST cycle can be approximated by a sine curve. While this is not true everywhere (sinus interpolation is problematic in some areas where non-linear feedbacks are acting e.g. Laepple and Lohmann, 2009) PRISM3D utilises a sine curve fit to February and August SST to generate twelve months of SST data. The formula first used for the mid-Pliocene by Dowsett et
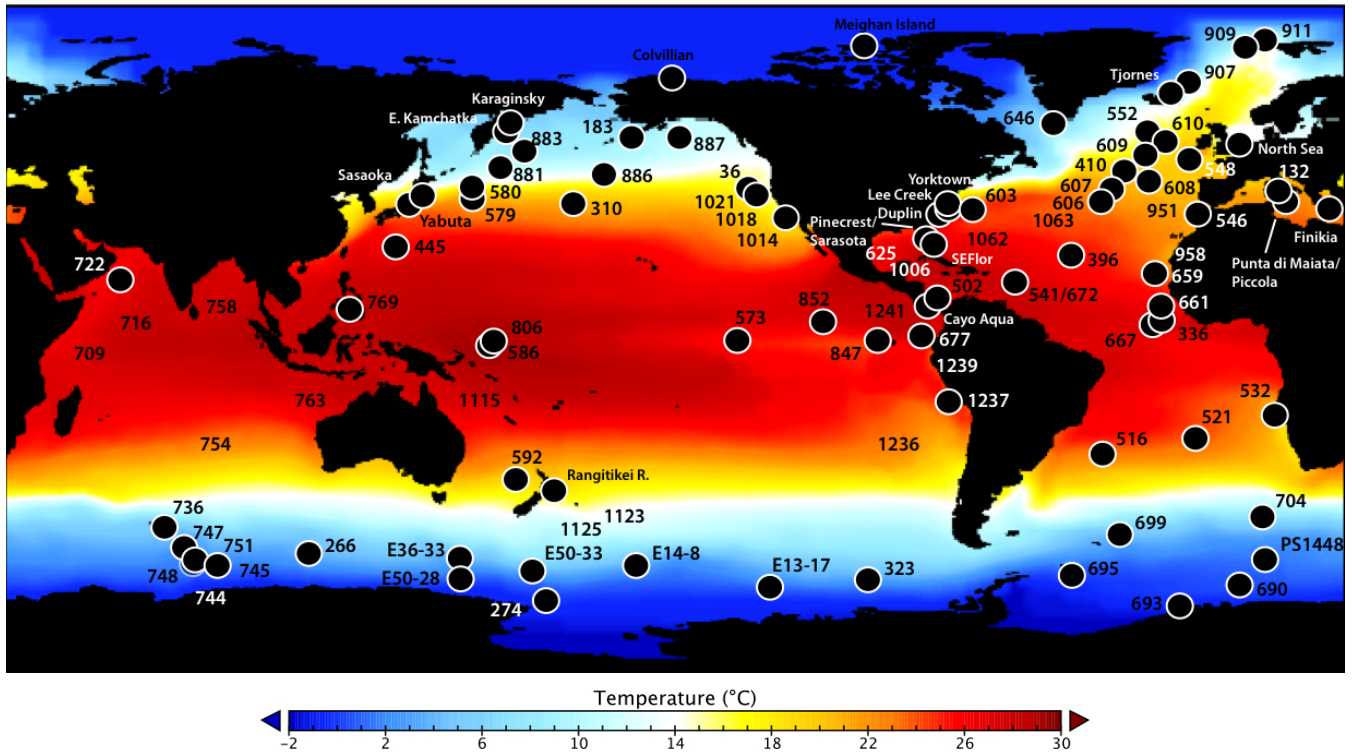
Fig. 8. PRISM3D mean annual SSTs and site localities.

al. (1994) to estimate monthly temperatures (*Tx*) other than February (*Ta*) and August (*Tf*) is:

$$ Tx = Tf + \frac{(Ta - Tf)}{2}\left(1 + \sin\left[\frac{2\pi (x-2)}{12} - \frac{\pi}{2}\right]\right). $$

The PRISM3D SST reconstruction shows little warming in low latitudes relative to late 20th century conditions, and increased warming at higher latitudes (Fig. 7). In the northern hemisphere the Kuroshio and Gulf Stream/North Atlantic Drift currents are regions of significant warm anomalies. Oceanographic fronts are generally displaced toward the polar regions and the zonally averaged pole to equator temperature gradient is reduced relative to present day.

3.4   Sea-ice extent

Sea-ice cover is part of the PRISM3D SST data set (Fig. 7). Southern Hemisphere sea-ice extent is determined by mid-Pliocene distribution of key diatom taxa (Barron, 1996a, b; Dowsett et al., 1996). Assuming an ice-free summer and maximum sea-ice extent governed by the diatom data, modern seasonal patterns of sea-ice waxing and waning were used to describe the Pliocene seasonal changes in sea ice. These data were further adjusted to fit available SST data in the Southern Ocean.

There is no direct evidence for mid-Pliocene sea ice extent in the northern hemisphere. However, extreme warmth documented in marine and terrestrial sequences in the Arctic argues for at least seasonally ice-free conditions (Brouwers, 1994; Cronin et al., 1993; Robinson 2009; Matthiessen et al., 2009). In a fashion similar to the method used in the Southern Hemisphere, modern seasonal growth patterns of sea-ice were used to expand and contract the ice margin from its mid-Pliocene maximum extent (=modern summer extent) to a summer ice-free condition. The mid-Pliocene maximum extent of sea ice (=modern summer extent) in both hemispheres is based upon SST reconstructions. Southern Ocean, North Atlantic/Arctic and North Pacific regions have Pliocene winter SST fields that resemble modern summer conditions. Assigning the modern minimum sea ice to the Pliocene winter therefore seems appropriate and in the Southern Ocean is further supported by diatoms and sedimentological data (Dowsett et al., 1994, 2009; Barron, 1996). Extreme warmth documented in the Arctic (Robinson, 2009) suggests seasonally ice-free conditions.

3.5   Vegetation type and distribution

The PRISM3D vegetation reconstruction is based on an approach which combines an internally consistent dataset of 202 palaeobotanical sites with predictions from a coupled
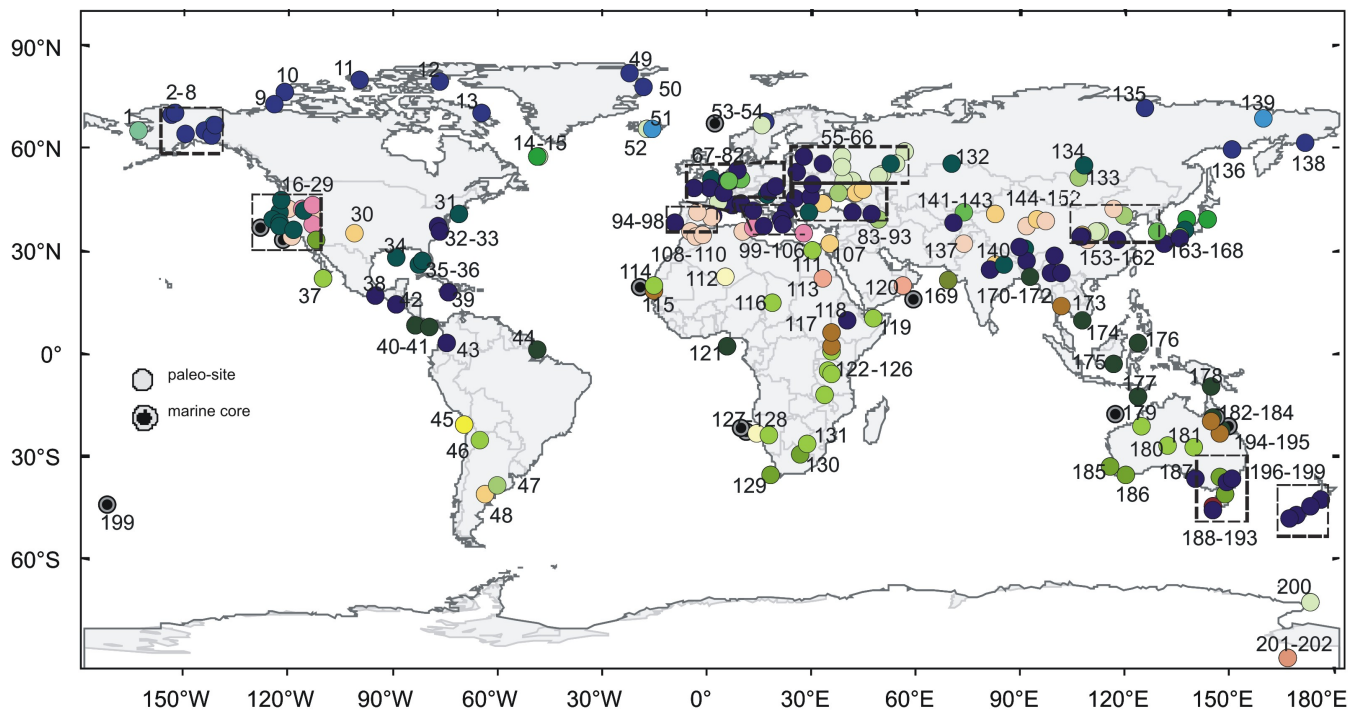
Fig. 9. Geographical distribution of 202 palaeobotanical sites used in the Salzmann et al. (2008) reconstruction of global Piacenzian Stage land cover.

climate-vegetation model (Fig. 9; Salzmann et al., 2008). By using the 28-biome classification scheme of the BIOME4 mechanistic model of vegetation (e.g. Prentice et al., 1992), the new Pliocene vegetation reconstruction is fully compatible with BIOME4 model outputs which facilitates comparison of proxy data and climate model/BIOME4 simulations. It is also more detailed than the previous PRISM2 vegetation reconstruction (Thompson and Fleming, 1996), which is based on a 7-type land cover classification scheme, palaeobotanical records from 74 sites and, in some cases, modern vegetation to fill data sparse regions. A full description of the new data-model hybrid and data-model coupling strategy including a complete list of palaeobotanical literature used for the biome reconstruction can be found in Salzmann et al. (2008).

In brief, Salzmann et al. (2008) compiled data from literature covering the Piacenzian stage (~3.6–2.6 Ma) and translated them into the BIOME4 scheme using the authors' interpretation taken from the original research paper. The greater time range compared to the SST data reflects the greater limitation/uncertainty in dating terrestrial sequences compared to marine sequences. A comprehensive GIS database was designed to synthesize and compare the output of our data-based biome reconstruction with predictions of the mechanistically based BIOME4 vegetation model forced by climatology derived from a standard mid-Pliocene Hadley Centre atmospheric model version 3 (HadAM3) GCM simulation (Haywood and Valdes, 2006). As the model simulation pro-

vides a much closer approximation to the true mid-Pliocene condition than modern vegetation, we used the BIOME4 output as a guide to interpolate and reconstruct vegetation for data-sparse regions.

The PRISM3D Pliocene vegetation reconstruction is available as a 28-type biome (Fig. 10) or a 9-type mega-biome map (Fig. 11) on a $2° \times 2°$ fractional land grid in netCDF or Excel spreadsheets format. Mega-biomes were classified after Harrison and Prentice (2003). The vegetation zonation reconstructed for the Piacenzian stage indicates a generally warmer and moister climate than today. Most prominent changes in biome distribution compared to today include a northward displaced evergreen taiga by more than 10 degrees, resulting in a significantly reduced area of tundra vegetation. The northward shift suggests that the polar regions were as an annual mean 10–15 °C warmer than today. The vegetation change was accompanied by a parallel northwards expansion of temperate forests and grasslands in Russia and eastern North America replacing boreal conifer forests. Further south, diverse warm-temperate forests with East Asian and North American affinities became dominant in central Europe. A wetter Pliocene climate also resulted in the expansion of tropical savannas and woodland in Africa and Australia at the expense of deserts.

By stating that modelling groups must change their vegetation to a mid-Pliocene state, PlioMIP will go beyond anything previously achieved within PMIP in which vegetation for the palaeo has always been specified as
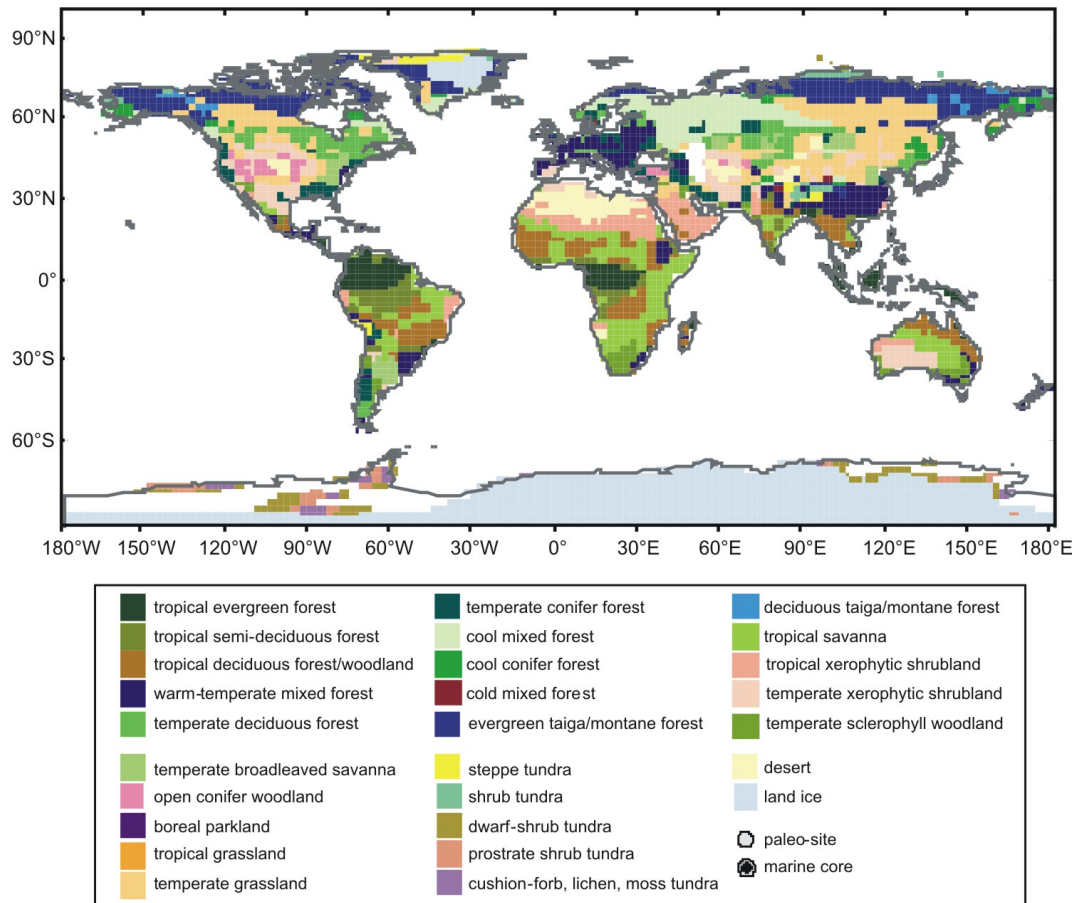
Fig. 10. The PRISM3D land cover data/model hybrid (Salzmann et al., 2008) displayed using the full BIOME4 classification scheme.

pre-industrial. This should aid the terrestrial data/model comparison but given the differences in the models land-surface schemes it is accepted that it will not be possible to ensure that each group provides the same forcing to each model even though the same vegetation data set it used. Individual groups must fully document with their papers for this GMD PlioMIP special issue how mid-Pliocene vegetation is implemented within their own models and should make sure that the procedure used to create a Pliocene vegetation map is self-consistent with their model's pre-industrial vegetation map (i.e. when using BIOME4-based modern vegetation, groups should be sure the procedure can adequately reproduce the pre-industrial vegetation map for their model). Note also that the pre-industrial vegetation data set used by each group should also include land-use, conforming to PMIP3/CMIP5 guidelines, to avoid the necessity of running a separate pre-industrial control simulation for PlioMIP as well as PMIP3/CMIP5.

To provide additional guidance we have produced a BIOME4 look up table which attempts to document how the BIOME4 full and mega-biome schemes relate to land surface physics as it is represented in The Hadley Centre Model version 3 (HadAM3 and HadCM3 running with version 1 of the Met Office Surface Exchange Scheme; Tables 2 and 3).

Each BIOME4 class was related to one or more land cover descriptions of Wilson and Henderson-Sellers (1999). Lookup-tables published in Wilson and Henderson-Sellers (1999) modified by Jones (unpublished) were used to calculate mean percentages of vegetation components (land cover description) and associated land cover class. If two or more land cover descriptions were used to describe a biome the average percentage for each land class was calculated and respective surface physics published in Cox et al. (1999). Mega-biomes were calculated by grouping and averaging physical surface parameters of relevant biomes.

3.6 River routing, soils and lakes

With regard to river routing, "preferred" and "alternate" solutions are specified. The preferred solution is to alter the river routes to follow the steepest gradient in mid-Pliocene topography. The alternate solution is to follow modern river routes except where inappropriate due to changes in the mid-Pliocene land/sea mask where rivers should be routed to the
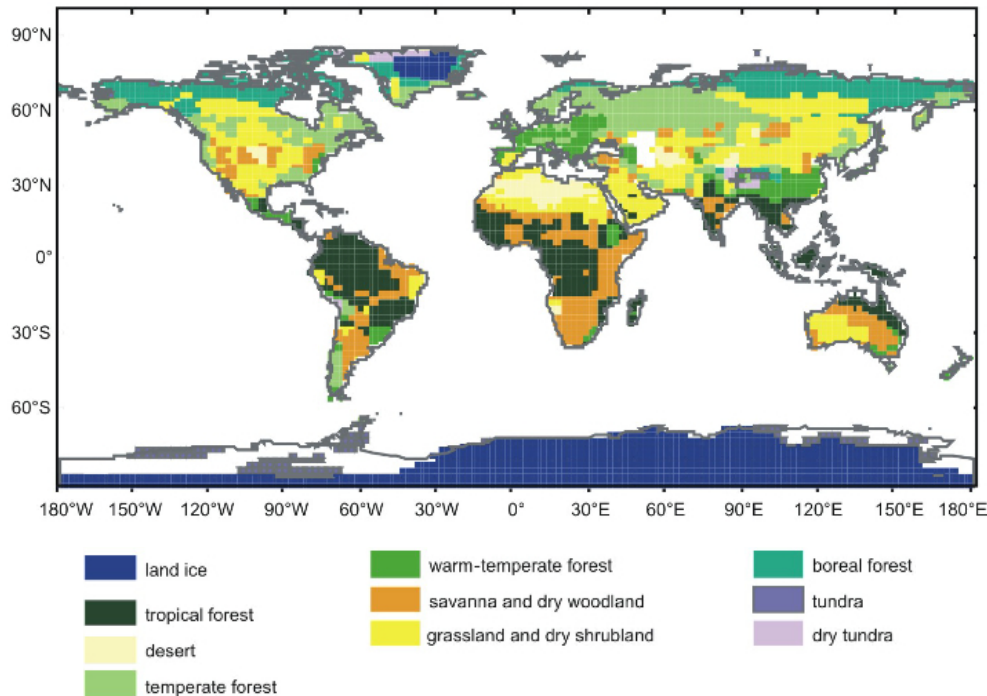
Fig. 11. The PRISM3D land cover data/model hybrid (Salzmann et al., 2008) displayed using the BIOME4 mega-biome scheme.

nearest ocean grid box. For soils two options are specified. Option 1 ("preferred") states that soil types and distribution can be specified in a way that is consistent with the imposed Pliocene vegetation distribution (see Sect. 3.6). Option 2 ("alternate") specifies soil types and distribution as modern. In areas where land has been created in the Pliocene reconstruction compared to the modern land/sea mask, soil type should be extrapolated from the nearest modern grid box.

In the PlioMIP experimental design lakes are specified as absent. The Salzmann et al. (2008) land cover reconstruction does not include any information on Piacenzian Stage lake distribution and/or size. Lake distributions will be incorporated into the PRISM4 version of the Salzmann et al. (2008) land cover reconstruction using a combination of collated sedimentary evidence and analyses of multi-model predicted mean annual Precipitation minus Evaporation balance (P-E; where a positive multi-model mean P-E indicates conditions suitable for the maintenance of lakes).

4   Variables, output format, data processing/storage, planned analyses

PlioMIP Phase 1 has adopted the established variables list outlined by the second phase of the PMIP project (Braconnot et al., 2007a, b). Model outputs will be submitted and stored within the PMIP2 database. Specifically, for PlioMIP Experiment 1, this refers to PMIP2 recommended outputs for the atmosphere (outlined on the PMIP2 website

http://pmip2.lsce.ipsl.fr/ > Experimental Design > Variables > Atmosphere). The PMIP/PlioMIP project requires participants to prepare their data files so that they meet the following constraints (regardless of the way their models produce and store their results).

– The data files have to be in the (now widely used) netCDF binary file format and conform to the CF (Climate and Forecast) metadata convention (outlined on the website http://cf-pcmdi.llnl.gov/).

– There must be only one output variable per file.

– For the data that are a function of longitude and latitude, only regular grids (grids representable as a Cartesian product of longitude and latitude axes) are allowed.

– The file names have to follow the PMIP2 file name convention and be unique.

Participants are encouraged to create the files for submission to the database using the CMOR library (Climate Model Output Rewriter). This library has been specially developed to help meet the requirements of the Model Intercomparison Projects. Details of the CMOR library are provided on the PMIP2 website (http://pmip2.lsce.ipsl.fr/ > Experimental design > Output format > CMOR library). Proposals for model analyses using PlioMIP Experiment 1 data can be made using the established protocols outlined on the PlioMIP website (http://geology.er.usgs.gov/eespteam/prism/prism_pliomip.html).

Table 2. BIOME4 land surface physics.

key	biome	rootdepth dr (m)	snow free albedo (α_0)	cold deep snow albedo (α_s)	surface resistance to evapo- ration rs (sm^{-1})	surface roughness length z_{0v} (m)	canopy water (surface) capacity c_m (mm)	vegetation infiltration enhance- ment I_v	leaf area index of vegetated fraction L	canopy height of vegetated h (m)	vegetation fraction
1	tropical evergreen forest	1.43E+00	1.21E-01	2.30E-01	1.29E+02	1.14E+00	6.90E-01	5.73E+00	8.58E+00	2.94E+01	9.50E-01
2	tropical semi-deciduous forest	1.43E+00	1.21E-01	2.30E-01	1.29E+02	1.14E+00	6.90E-01	5.73E+00	8.58E+00	2.94E+01	9.50E-01
3	tropical deciduous forest/woodland	6.96E-01	1.37E-01	4.36E-01	9.76E+01	6.85E-01	5.92E-01	3.06E+00	4.85E+00	1.28E+01	8.00E-01
4	temperate deciduous forest	1.08E+00	1.36E-01	3.55E-01	9.60E+01	8.51E-01	5.85E-01	5.28E+00	4.68E+00	1.34E+01	9.50E-01
5	temperate conifer forest	8.40E-01	1.36E-01	2.55E-01	8.45E+01	9.01E-01	1.13E+00	5.50E+00	5.79E+00	1.81E+01	9.50E-01
6	warm-temperate mixed forest	9.75E-01	1.31E-01	3.00E-01	9.13E+01	9.00E-01	8.60E-01	5.50E+00	5.32E+00	1.61E+01	9.50E-01
7	cool mixed forest	9.75E-01	1.31E-01	3.00E-01	9.13E+01	9.00E-01	8.60E-01	5.50E+00	5.32E+00	1.61E+01	9.50E-01
8	cool conifer forest	8.40E-01	1.36E-01	2.55E-01	8.45E+01	9.01E-01	1.13E+00	5.50E+00	5.79E+00	1.81E+01	9.50E-01
9	cold mixed forest	9.75E-01	1.31E-01	3.00E-01	9.13E+01	9.00E-01	8.60E-01	5.50E+00	5.32E+00	1.61E+01	9.50E-01
10	evergreen taiga/ montane forest	8.40E-01	1.36E-01	2.55E-01	8.45E+01	9.01E-01	1.13E+00	5.50E+00	5.79E+00	1.81E+01	9.50E-01
11	deciduous taiga/ montane forest	8.40E-01	1.27E-01	3.45E-01	8.45E+01	9.01E-01	9.50E-01	5.50E+00	3.89E+00	9.49E+00	9.50E-01
12	tropical savanna	8.30E-01	1.76E-01	5.30E-01	9.10E+01	2.70E-01	6.90E-01	2.73E+00	5.05E+00	6.82E+00	9.50E-01
13	tropical xerophytic shrubland	6.90E-01	1.86E-01	5.90E-01	8.55E+01	1.64E-01	7.30E-01	2.18E+00	4.06E+00	2.69E+00	8.50E-01
14	temperate xerophytic shrubland	6.80E-01	1.76E-01	5.95E-01	7.80E+01	2.43E-01	8.00E-01	2.25E+00	2.71E+00	1.32E+00	9.00E-01
15	temperate sclerophyll woodland	9.10E-01	1.48E-01	4.60E-01	8.90E+01	6.02E-01	6.75E-01	4.03E+00	3.94E+00	8.82E+00	9.00E-01
16	temperate broad-leaved savanna	9.20E-01	1.51E-01	4.55E-01	8.70E+01	6.23E-01	5.85E-01	4.23E+00	3.95E+00	9.63E+00	9.50E-01
17	open conifer woodland	7.00E-01	1.57E-01	4.10E-01	7.90E+01	6.03E-01	9.20E-01	4.10E+00	4.67E+00	1.29E+01	9.00E-01
18	boreal parkland	7.00E-01	1.57E-01	4.10E-01	7.90E+01	6.03E-01	9.20E-01	4.10E+00	4.67E+00	1.29E+01	9.00E-01
19	tropical grassland	6.90E-01	1.79E-01	5.90E-01	8.55E+01	1.64E-01	7.30E-01	2.18E+00	4.06E+00	2.69E+00	8.50E-01
20	temperate grassland	4.78E-01	1.89E-01	6.99E-01	6.64E+01	2.92E-02	5.31E-01	1.47E+00	2.13E+00	4.88E-01	8.80E-01
21	desert	1.60E-01	2.5E-01	7.73E-01	9.80E+01	3.13E-02	5.43E-01	7.25E-01	2.75E+00	1.33E+00	1.00E-01
22	steppe tundra	1.60E-01	1.50E-01	8.00E-01	7.60E+01	4.18E-03	5.80E-01	7.00E-01	1.00E+00	1.00E+00	4.00E-01
23	shrub tundra	5.60E-01	1.59E-01	6.50E-01	6.60E+01	2.04E-01	8.30E-01	1.95E+00	2.11E+00	1.39E+00	9.00E-01
24	dwarf-shrub tundra	1.60E-01	1.50E-01	8.00E-01	7.60E+01	4.18E-03	5.80E-01	7.00E-01	1.00E+00	1.00E+00	4.00E-01
25	prostrate shrub tundra	1.60E-01	1.50E-01	8.00E-01	7.60E+01	4.18E-03	5.80E-01	7.00E-01	1.00E+00	1.00E+00	4.00E-01
26	cushion-forb, lichen, moss tundra	1.60E-01	1.50E-01	8.00E-01	7.60E+01	4.18E-03	5.80E-01	7.00E-01	1.00E+00	1.00E+00	4.00E-01
27	barren (soil)	1.00E-01	n/a	8.00E-01	1.00E+02	3.00E-04	5.00E-01	5.00E-01	0.00E+00	0.00E+00	0.00E+00
28	land ice	0.00E+00	7.50E-01	8.00E-01	0.00E+00	1.00E-04	0.00E+00	0.00E+00	0.00E+00	0.00E+00	0.00E+00

5 Conclusions

This paper has provided a detailed model intercomparison project description for the Pliocene Model Intercomparison Project (PlioMIP) and documents in detail the experimental design. Specifically, this paper described the experimental design and boundary conditions utilised for Experiment 1 of PlioMIP and will be followed by a companion paper for Experiment 2 in the PlioMIP special issue of GMD.

Table 3. BIOME4 land surface physics (mega-biomes).

key	mega-biome	rootdepth dr	snow free albedo	cold deep snow albedo	surface resistance to evaporation rs	surface roughness length z_{0v}	canopy water (surface) capacity c_m	vegetation infiltration enhancement I_v	leaf area index of vegetated fraction L	canopy height of vegetated h	vegetation fraction
		(m)	(α_0)	(α_s)	(sm^{-1})	(m)	(mm)			(m)	
1	tropical forest	1.43E+00	1.21E-01	2.30E-01	1.29E+02	1.14E+00	6.90E-01	5.73E+00	8.58E+00	2.94E+01	9.50E-01
2	warm-temperate forest	9.75E-01	1.31E-01	3.00E-01	9.13E+01	9.00E-01	8.60E-01	5.50E+00	5.32E+00	1.61E+01	9.50E-01
3	savanna and dry woodland	8.39E-01	1.53E-01	4.70E-01	9.12E+01	5.45E-01	6.36E-01	3.51E+00	4.45E+00	9.52E+00	9.00E-01
4	grassland and dry shrubland	6.35E-01	1.83E-01	6.19E-01	7.89E+01	1.50E-01	6.98E-01	2.02E+00	3.24E+00	1.80E+00	8.70E-01
5	desert	1.60E-01	2.5E-01	7.73E-01	9.80E+01	3.13E-02	5.43E-01	7.25E-01	2.75E+00	1.33E+00	1.00E-01
6	temperate forest	1.01E+00	1.33E-01	3.18E-01	9.29E+01	8.84E-01	7.68E-01	5.43E+00	5.11E+00	1.52E+01	9.50E-01
7	boreal forest	7.70E-01	1.44E-01	3.55E-01	8.18E+01	7.52E-01	9.80E-01	4.80E+00	4.76E+00	1.33E+01	9.25E-01
8	tundra	1.60E-01	1.50E-01	8.00E-01	7.60E+01	4.18E-03	5.80E-01	7.00E-01	1.00E+00	1.00E+00	4.00E-01
9	dry tundra	1.60E-01	1.50E-01	8.00E-01	7.60E+01	4.18E-03	5.80E-01	7.00E-01	1.00E+00	1.00E+00	4.00E-01
28	land ice	0.00E+00	7.50E-01	8.00E-01	0.00E+00	1.00E-04	0.00E+00	0.00E+00	0.00E+00	0.00E+00	0.00E+00

References

Barron, J. A.: Pliocene paleoclimatic interpretation of DSDP site 580 (NW Pacific) using diatoms, Mar. Micropaleontol., 20, 23–44, 1992.

Barron, E. J. and Washington, W. M.: Cretaceous Climate: A Comparison of Atmospheric Simulations with the Geologic Record, Palaeogeogr. Palaeocl., 40, 103–133, 1982.

Barron, J. A.: Diatom constraints on the position of the Antarctic Polar Front in the middle part of the Pliocene, Mar. Micropaleontol., 27, 195–213, 1996a.

Barron, J. A.: Diatom constraints on sea surface temperatures and sea ice distribution during the middle part of the Pliocene, US Geol. Surv., Open File Rep. 96–713, 45 pp., 1996b.

Berggren, W. A., Kent, D. V., Swisher, C. C., and Aubry, M. P.: A revised Cenozoic geochronology and chronostratigraphy, in: Geochronology, time scales and global stratigraphic correlation, edited by: Berggren, W. A., Kent, D. V., Aubry, M. P., and Hardenbol, J., Tulsa, Soc. Sed. Geol., Spec. Pub. 54, 129–212, 1995.

Braconnot, P., Otto-Bliesner, B., Harrison, S., Joussaume, S., Peterchmitt, J.-Y., Abe-Ouchi, A., Crucifix, M., Driesschaert, E., Fichefet, Th., Hewitt, C. D., Kageyama, M., Kitoh, A., Laˆné, A., Loutre, M.-F., Marti, O., Merkel, U., Ramstein, G., Valdes, P., Weber, S. L., Yu, Y., and Zhao, Y.: Results of PMIP2 coupled simulations of the Mid-Holocene and Last Glacial Maximum - Part 1: experiments and large-scale features, Clim. Past, 3, 261–277, 2007a,
http://www.clim-past.net/3/261/2007/.

Braconnot, P., Otto-Bliesner, B., Harrison, S., Joussaume, S., Peterchmitt, J.-Y., Abe-Ouchi, A., Crucifix, M., Driesschaert, E., Fichefet, Th., Hewitt, C. D., Kageyama, M., Kitoh, A., Loutre, M.-F., Marti, O., Merkel, U., Ramstein, G., Valdes, P., Weber, L., Yu, Y., and Zhao, Y.: Results of PMIP2 coupled simulations of the Mid-Holocene and Last Glacial Maximum – Part 2: feedbacks with emphasis on the location of the ITCZ and mid- and high latitudes heat budget, Clim. Past, 3, 279–296, 2007b,
http://www.clim-past.net/3/279/2007/.

Brouwers, E. M.: Late Pliocene paleoecologic reconstructions based on ostracode assemblages from the Sagavanirktok and Gubik formations, Alaskan north slope, Arctic, 47, 16–33, 1994.

Cox, P. M., Betts, R. A., Bunton, C. B., Essery, R. L. H., Rowntree, P. R., and Smith, J.: The impact of new land surface physics on the GCM simulation of climate and climate sensitivity, Clim. Dynam., 15, 183–203, 1999.

Cronin, T. M.: Pliocene shallow water paleoceanography of the North Atlantic ocean based on marine ostracodes, Quaternary Sci. Rev., 10, 175–188, doi:10.1016/0277-3791(91)90017-O, 1991.

Cronin, T. M., Whatley, R., Wood, A., Tsukagoshi, A., Ikeya, N., Brouwers, E. M., and Briggs Jr., W. M.: Microfaunal evidence for elevated Pliocene temperatures in the arctic ocean, Paleoceanography, 8, 161–173, doi:10.1029/93PA00060, 1993.

DeConto, R. M. and Pollard, D.: Rapid Cenozoic glaciation of Antarctica induced by declining atmospheric CO_2, Nature, 421, 245–249, 2003.

Dowsett, H. J.: The PRISM palaeoclimate reconstruction and Pliocene sea-surface temperature, in: Deep-time perspectives on climate change: Marrying the signal from computer models and biological proxies, edited by: Williams, M., Haywood, A. M., Gregory, J., and Schmidt, D. N., Micropalaeontological Soc., Spec. Pub., Geol. Soc. of London, London, UK, 459–480, 2007a.

Dowsett, H. J.: Faunal re-evaluation of mid-Pliocene conditions in the western equatorial pacific, Micropaleontology, 53, 447–456, 2007b.

Dowsett, H. J. and Cronin, T. M.: High eustatic sea level during the middle Pliocene: Evidence from the southeastern U.S. Atlantic coastal plain, Geology, 18, 435–438, 1990.

Dowsett, H. J. and Loubere, P.: High resolution late Pliocene sea-surface temperature record from the northeast Atlantic ocean, Mar. Micropaleontol., 20, 91–105, doi:10.1016/0377-8398(92)90001-Z, 1992.

Dowsett, H. J. and Poore, R. Z.: A new planktic foraminifer transfer function for estimating Pliocene-Holocene palaeoceanographic conditions in the North Atlantic, Mar. Micropaleontol., 16, 1–24, 1990.

Dowsett, H. J. and Poore, R. Z.: Pliocene sea surface temperatures of the North Atlantic ocean at 3.0 Ma, Quaternary Sci. Rev., 10, 189–204, doi:10.1016/0277-3791(91)90018-P, 1991.

Dowsett, H. J. and Robinson, M. M.: Stratigraphic framework for Pliocene paleoclimate reconstruction: The correlation conundrum, Stratigraphy, 3, 53–64, 2006.

Dowsett, H. J. and Robinson, M. M.: Mid-Pliocene equatorial pacific sea surface temperature reconstruction: A multi-proxy perspective, Philos. T. R. Soc. A., 367, 109–125, doi:10.1098/rsta.2008.0206, 2009.

Dowsett, H. J., Barron, J., and Poore, H. R.: Middle Pliocene sea surface temperatures: A global reconstruction, Mar. Micropaleontol., 27, 13–25, doi:10.1016/0377-8398(95)00050-X, 1996.

Dowsett, H. J., Barron, J. A., Poore, R. Z., Thompson, R. S., Cronin, T. M., Ishman, S. E., and Willard, D. A.: Middle Pliocene paleoenvironmental reconstruction: PRISM 2, US Geol. Surv., Open File Rep., 99–535, 1999.

Dowsett, H. J., Chandler, M. A., and Robinson, M. M.: Surface temperatures of the mid-Pliocene North Atlantic ocean: Implications for future climate, Philos. T. R. Soc. A, 367, 69–84, doi:10.1098/rsta.2008.0213, 2009a.

Dowsett, H. J., Cronin, T. M., Poore, R. Z., Thompson, R. S., Whatley, R. C., and Wood, A. M.: Micropaleontological evidence for increased meridional heat transport in the North Atlantic ocean during the Pliocene, Science, 258, 1133–1135, 10.1126/science.258.5085.1133, 1992.

Dowsett, H. J., Robinson, M. M., and Foley, K. M.: Pliocene three-dimensional global ocean temperature reconstruction, Clim. Past, 5, 769–783, 2009b,
http://www.clim-past.net/5/769/2009/.

Dowsett, H. J., Thompson, R. S., Barron, J. A.. Cronin, T. M., Fleming, R. F., Ishman, E., Poore, R. Z., Willard, D. A., and Holtz, T. R.: Joint investigations of the middle Pliocene climate I: PRISM paleoenvironmental reconstructions, Global Planet. Change, 9(4), 169–195, 1994.

Garzione, C. N., Molnar, P., Libarkin, J. C., and MacFadden, B. J.: Rapid late Miocene rise of the Bolivian Altiplano-Evidence for removal of mantle lithosphere, Earth Planet. Sci. Lett., 241, 543–556, 2006.

Ghosh, P., Garzione, C. N., and Eiler, J. M.: Rapid uplift of the Altiplano revealed through 13C–18O bonds in paleosol carbonates, Science, 311, 511–515, 2006.

Gordon, C., Cooper, C., Senior, C. A., Banks, H., Gregory, J. M., Johns, T. C., Mitchell, J. F. B., and Wood, R. A.: The simulation of SST, sea ice extents and ocean heat transports in a version of the Hadley Centre coupled model without flux adjustments, Clim. Dynam., 16, 147–168, 2000.

Harrison, S. P. and Prentice, I. C.: Climate and CO_2 controls on global vegetation distribution at the last glacial maximum: analysis based on palaeovegetation data, biome modelling and palaeoclimate simulations, Glob. Change Biol., 9, 983–1004, 2003.

Haywood, A. M. and Valdes, P. J.: Vegetation cover in a warmer world simulated using a dynamic global vegetation model for the Mid-Pliocene, Palaeogeogr. Palaeocl., 237, 412–427, 2006.

Haywood, A. M., Chandler, M. A., Valdes, P. J., Salzmann, U., Lunt, D. J., and Dowsett, H. J.: Comparisons of mid-Pliocene climate predictions produced by the HadAM3 and GCMAM3 General Circulation Models, Global Planet. Change, 66, 208–224, 2009.

Haywood, A. M., Valdes, P. J., and Peck, V. L.: A permanent El Niño-like state during the Pliocene?, Paleoceanography, 22, PA1213, doi:10.1029/2006PA001323, 2007.

Hill, D. J., Haywood, A. M., Hindmarsh, R. C. M., and Valdes, P. J.: Characterising ice sheets during the Pliocene: evidence from data and models, in: Deep-time perspectives on climate change: marrying the signal from computer models and biological proxies, edited by: Williams, M., Haywood, A. M., Gregory, J., and Schmidt, D., Micropalaeontol. Soc., Spec. Pub. Geol. Soc., London, 517–538, 2007.

Hill, D. J.: Modelling Earth's Cryosphere during Pliocene Warm Peak, Ph.D. thesis, University of Bristol, UK, 368 pp., 2009.

Hoar, M. R., Palutikof, J. P., and Thorne, M. C.: Model intercomparison for the present day, the mid-Holocene, and the Last Glacial Maximum over Western Europe, J. Geophys. Res., 109, D08104, doi:10.1029/2003JD004161, 2004.

Hodell, D. A. and Ciesielski, P. F.: Stable isotopic and carbonate stratigraphy of the Plio-Pleistocene of Ocean Drilling Program (ODP) hole 704a: Eastern subantarctic South Atlantic, Proceedings of the Ocean Drilling Program Scientific Results, 114, 409–436, 1991.

Huber, M. and Caballero, R.: Eocene El Niño: Evidence for robust tropical dynamics in the "Hothouse", Science, 299, 877–881, 2003.

Joussaume, S. and Taylor, K. E.: Status of the Paleoclimate Modeling Intercomparison Project (PMIP), Proceedings of the first international AMIP scientific conference, WCRP Report, 425–430, 1995.

Kim, S. J. and Crowley, T. J.: Increased Pliocene North Atlantic Deep Water – Cause or consequence of Pliocene warming?, Paleoceanography, 15, 451–455, 2000.

Krantz, D. E.: A chronology of Pliocene sea level fluctuations: The U.S. middle Atlantic Coastal Plain record, Quaternary Sci. Rev., 10, 163–174, 1991.

Kürschner, W. M., Van der Burgh, J., Visscher, H., and Dilcher, D. L.: Oak leaves as biosensors of late Neogene and early Pleistocene paleoatmospheric CO_2 concentrations, Mar. Micropaleontol., 27(1/4), 299–312, 1996.

Kutzbach, J. E. and Otto-Bliesner, B. L.: The Sensitivity of the African-Asian Monsoonal Climate to Orbital Parameter Changes for 9000 yr B.P. in a Low-resolution General Circulation Model, J. Atmos. Sci., 39, 1177–1188, 1982.

Laepple, T. and Lohmann, G.: The seasonal cycle as template for climate variability on astronomical time scales, Paleoceanography, 24, PA4201, doi:10.1029/2008PA001674, 2009.

Laskar, J., Robutel, P., Joutel, F., Gastineau, M., Correia, A. C. M., and Levrard, B.: A long term numerical solution for the insolation quantities of the Earth, Astron. Astrophys., 428, 261–285, doi:10.1051/0004-6361:20041335, 2004.

Lisiecki, L. E. and Raymo, M. E.: A Pliocene-Pleistocene stack of 57 globally distributed benthic $\delta^{18}O$ records, Paleoceanography, 20, PA1003, 10.1029/2004PA001071, 2005.

Loulergue, L., Schilt, A., Spahni, R., Masson-Delmotte, V., Blunier, T., Lemieux, B., Barnola, J. M., Raynaud, D., Stocker, T. F., and Chappellaz, J.: Orbital and millennial-scale features of atmospheric CH_4 over the past 800 000 years, Nature, 453, 383–386, 2008.

Lüthi, D., Le Floch, M., Bereiter, B., Blunier, T., Barnola, J.-M., Siegenthaler, U., Raynaud, D., Jouzel, J., Fischer, H., Kawamura, K., and Stocker, T. F.: High-resolution carbon dioxide concentration record 650 000–800 000 years before present, Nature, 453, 379–382, 2008.

Markwick, P. J.: The palaeogeographic and palaeoclimatic significance of climate proxies for data-model comparisons, in: Deep-time perspectives on climate change: marrying the signal from computer models and biological proxies, edited by: Williams, M., Haywood, A. M., Gregory, J., and Schmidt, D., Micropalaeontol. Soc., Spec. Pub. Geol. Soc., London, 251–312, 2007..

Matthews Jr., J. V. and Ovenden, L. E.: Late Tertiary plant macrofossils from localities in Arctic/subarctic North America: A review of the data, Arctic, 43, 364–392, 1990.

Matthiessen, J., Knies, J., Vogt, C., and Stein, R.: Pliocene palaeoceanography of the Arctic Ocean and subarctic seas, Philos. T. R. Soc. A, 367, 21–48, doi:10.1098/rsta.2008.0203, 2009.

McMillan, M. E., Heller, P. L., and Wing, S. L.: History and causes of post-Laramide relief in the Rocky Mountain orogenic plateau, Geol. Soc. Am. Bull., 118, 393–405, doi:10.1130/B25712.1, 2006.

Naish, T., Powell, R., Levy, R., Wilson, G., Scherer, R., Talarico, F., Krissek, L., Niessen, F., Pompilio, M., Wilson, T., Carter, L., DeConto, R., Huybers, P., McKay, R., Pollard, D., Ross, J., Winter, D., Barrett, P., Browne, G., Cody, R., Cowan, E., Crampton, J., Dunbar, G., Dunbar, N., Florindo, F., Gebhardt, C., Graham, I., Hannah, M., Hansaraj, D., Harwood, D., Helling, D., Henrys, S., Hinnov, L., Kuhn, G., Kyle, P., Laufer, A., Maffioli, P., Magens, D., Mandernack, K., McIntosh, W., Millan, C., Morin, R., Ohneiser, C., Paulsen, T., Persico, D., Raine, I., Reed, J., Riesselman, C., Sagnotti, L., Schmitt, D., Sjunneskog, C., Strong, P., Taviani, M., Vogel, S., Wilch, T., and Williams, T.: Obliquity-paced Pliocene West Antarctic ice sheet oscillations, Nature, 458, 322–328, 2009

NOAA: Data Announcement 88-MGG-02, Digital Relief of the Surface of the Earth, 1988.

Otto-Bliesner, B., Harrison, S. P., Joussaume, S., Abe-Ouchi, A., and Braconnot, P.: PMIP2 Workshop Report, Estes Park, USA, 15–19 September 2008, PAGES News, 17, 42–43, 2009.

Pollard, D. and DeConto, R. M.: Modelling West Antarctic ice sheet growth and collapse through the past five million years, Nature, 458, 329–332, 2009.

Prentice, I. C., Cramer, W., Harrison, S. P., Leemans, R., Monserud, R. A., and Solomon, A. M.: A global biome model based on plant physiology and dominance, soil properties and climate, J. Biogeogr., 19, 117–134, 1992.

Prentice, I. C. and Webb III, T.: BIOME 6000: reconstructing global mid-Holocene vegetation patterns from palaeoecological records, J. Biogeogr., 25, 997–1005, 1998.

Randall, D. A., Wood, R. A., Bony, S., Colman, R., Fichefet, T., Fyfe, J., Kattsov, V., Pitman, A., Shukla, J., Srinivasan, J., Stouffer, R. J., Sumi, A. and Taylor, K. E.: Climate Models and Their Evaluation, in: Climate Change 2007: The Physical Science Basis, edited by: Solomon, S., Qin, D., Manning, M., Marquis, M., Averyt, K., Tignor, M. M. B., Miller Jr., H. L., and Chen, Z., Cambridge University Press, 2007.

Raymo, M. E., Grant, B., Horowitz, M., and Rau, G. H.: Mid-Pliocene warmth: Stronger greenhouse and stronger conveyor, Mar. Micropaleontol., 27, 313–326, 10.1016/0377-8398(95)00048-8, 1996.

Raymo, M. E., Ruddiman, W. F., Backman, J., Clement, B. M., and Martinson, D. G.: Late Pliocene variation in northern hemisphere ice sheets and North Atlantic deep water circulation, Paleoceanography, 4, 413-446, 10.1029/PA004i004p00413, 1989.

Reynolds, R. W. and Smith, T. M.: A high-resolution global sea surface temperature climatology, J. Climate, 8, 1571–1583, 1995.

Robinson, M. M.: New quantitative evidence of extreme warmth in the Pliocene Arctic, Stratigraphy, 6(4), 265–275, 2009.

Robinson, M. M., Dowsett, H. J., Dwyer, G. S., and Lawrence, K. T.: Reevaluation of mid-Pliocene North Atlantic sea surface temperatures, Paleoceanography, 23, PA3213, doi:10.1029/2008PA001608, 2008.

Rowley, D. B. and Garzione, C. N.: Stable isotope-based paleoaltimetry, Annu. Rev. Earth Pl. Sc., 35, 463–508, doi:10.1146/annurev.earth.35.031306.140155, 2007.

Sancetta, C. and Silvestri, S.: Pliocene-Pleistocene evolution of the North Pacific ocean-atmosphere system, interpreted from fossil diatoms, Paleoceanography, 1, 163–180, doi:10.1029/PA001i002p00163, 1986.

Salzmann, U., Haywood, A. M., Lunt D. J., Valdes, P. J., and Hill, D. J.: A new Global Biome Reconstruction and Data-Model Comparison for the middle Pliocene, Global Ecol. Biogeogr., 17, 432–447, 2008.

Shackleton, N. J., Crowhurst, S., Hagelberg, T., Pisias, N. G., and Schneider, D. A.: A new Late Neogene time scale: Application to Leg 138 sites, Proc. ODP Sci. Results, 73–101, 1995.

Sohl, L. E. and Chandler, M. A.: Reconstructing Neoproterozoic paleoclimates using a combined data/modelling approach, in: Deep-time perspectives on climate change: marrying the signal from computer models and biological proxies, edited by: Williams, M., Haywood, A. M., Gregory, J., and Schmidt, D., Micropalaeontol. Soc., Spec. Pub. Geol. Soc., London, 61–80, 2007.

Sohl, L. E., Chandler, M. A., Schmunk, R. B., Mankoff, K., Jonas, J. A., Foley, K. M., and Dowsett, H. J.: PRISM3/GISS topographic reconstruction, U. S. Geol. Surv. Data Series, 419, 6 pp., 2009.

Solomon, S., Qin, D., Manning, M., Marquis, M., Averyt, K., Tignor, M. M. B., Miller Jr., H. L., and Chen, Z. (Eds.): Climate Change 2007: The Physical Science Basis, Cambridge University Press, 2007.

Thompson, R. S. and Fleming, R. F.: Middle Pliocene vegetation: reconstructions, paleoclimatic inferences, and boundary conditions for climate modeling, Mar. Micropaleontol., 27, 27–49, 1996.

Valdes, P. J. and Sellwood, B. W.: A palaeoclimate model for the Kimmeridgian, Palaeogeogr. Palaeocl., 95, 47–72, 1992.

Vieli, A. and Payne, A. J.: Assessing the ability of numerical ice sheet models to simulate grounding line migration, J. Geophys. Res., 110, F01003, doi:10.1029/2004JF000202, 2005.

Williams, M., Haywood, A. M., Gregory, J., and Schmidt, D. (Eds.): Deep-time perspectives on climate change: marrying the signal from computer models and biological proxies, Micropalaeontol. Soc., Spec. Pub. Geol. Soc., London, 2007.

Webb, P.-N. and Harwood, D. M.: Late cenozoic glacial history of the Ross Embayment, Antarctica, Quaternary Sci. Rev., 10, 215–223, doi:10.1016/0277-3791(91)90020-U, 1991.

Wilson, M. F. and Henderson-Sellers, A.: A Global Archive of Land Cover and Soils Data for Use in General Circulation Climate Models, J. Climatol., 5, 119–143, 1985.

Zheng, W., Braconnot, P., Guilyardi, E., Merkel, U., and Yu, Y.: ENSO at 6ka and 21 ka from ocean-atmosphere coupled model simulations, Clim. Dynam., 30, 745–762, 2008.